# FATIGUE ANALYSIS OF FIBER-REINFORCED CEMENT TREATED BASES

*Coni M.*
*Associate Professor – University of Cagliari. – mconi@unica.it*

*Pani S.*
*Engineer – panising@tiscali.it*

## ABSTRACT

This paper reports the experimental results and theoretical fatigue analysis carried out on fiber-reinforced cemented base to predict the semi-rigid pavement performance. In the first phase, 18 split tensile tests were performed under different cement content (0%, 2.5%, and 3.5%) and steel fiber content (0%, 0.75%, and 1.5%). In June of 2002, two different test sections were build in south-east Sardinia, using conventional construction techniques and equipment, to evaluate the effectiveness of in-place mixing of composite materials and to quantify the effects of the fibers during the life service of the pavement. A fatigue analysis was developed using experimental results and a theoretical model of cement concrete, based on the comparison of the hysteretic envelope of load cycles and the □□curve in tension. Finally, a chemical test was carried out in order to evaluate the corrosion phenomena on the fiber-reinforcement used in the base cement layer

*Keywords: Cemented base; Fatigue; Fiber-Reinforce*

# 1. INTRODUCTION

The mechanical behavior of metallic fibers inside semi-rigid pavement has not been fully researched yet. The difficulties associated with behavior characterization may be attributed to the different response of the cement treated bases during their service life. Before cracking, the performance of the material is similar to that of a rigid layer with flexural stiffness. Afterwards, due to drying contraction, applied loads, and stress thermal cycles, a general cracking occurs. A low cement content causes less cracking, but as the quantity of cement increases, cracks increase in expansion, distance and aperture. The Young's modulus also increases with increasing cement content, thereby increasing the stress level in the material, without it having sufficient resistance characteristics. Therefore, the result is that of a latent cracking which starts during the initial phases of spreading and ageing. Its extension and evolution will depend strictly on the thermal and hygrometric conditions and on the working traffic loads. The number and intensity of traffic loads lead to a fatigue phenomena which is directly connected to the fragility of the material. The performance improvement of cement treated bases is subsequent to the enhancement of the characteristics of tensile resistance, especially during the first phases of the laying of the material and during the first and second year of service life. A promising technology is that of achieving such improvement introducing steel fibers. The paper first presents the results of the experimental tests carried out in the laboratory on fiber-reinforced cement treated bases and their use in a semi-rigid pavement in a section of a state road. The paper then illustrates the expected fatigue performance for such materials, through the modification of a valid model for the cement concrete. The final section of the paper analyzes the results of chemical tests on unused fibers, with the aim of assessing the actual risk of their corrosion inside the composite material in the experimental road section.

# 2. EXPERIMENTAL PROGRAM

The study was based on the analysis of the performance of 18 samples submitted to indirect tensile tests. Test combinations included two different quantities of cement (2.5% and 3.5%) and three different quantities of fiber (0%, 0.75%, and 1.5%). For each specimen combination, tests were performed in triplicate, on 3 samples, with the result being averaged. Each specimen was marked according to the following scheme:

**Table 1 Content of fibers and cement of the specimens**

| **Material** | **A** | **B** | **C** | **D** | **E** | **F** |
|---|---|---|---|---|---|---|
| **Cement %** | 2.5 | 3.5 | 2.5 | 3.5 | 2.5 | 3.5 |
| **Fiber** % | 0 | 0 | 0.75 | 0.75 | 1.50 | 1.50 |

The aggregate in all treated materials was crushed material, with maximun size of 40 mm. Table 2 shows the grading distribution of the aggregate.

**Table 2 Grading of treated materials**

| **Size [mm]** | 0.075 | 0.18 | 0.4 | 2 | 5 | 10 | 15 | 25 | 30 | 40 |
|---|---|---|---|---|---|---|---|---|---|---|
| **%** | 7.13 | 10.39 | 15.23 | 28.63 | 35.31 | 52.57 | 65.92 | 76.03 | 88.11 | 100 |

The cement content was kept low deliberately in specimens A, C and E, in order to underline the effect of the fiber. The use of fibers has been experimented with broadly in traditional concrete and mortars. In recent years, this led to the definition of standard methods of analysis and testing. Nevertheless, these methods cannot be used on fiber-reinforced cement treated bases for roads, which therefore are lacking in adequate regulatory framework. In Italy, the specification for standard testing requires compaction of cylindrical specimens with different quantities of cement and water. After 24 hours, the specimens are extracted and set for 6 days in a humid environment (90%), and then submitted to indirect tensile tests (> 0.25-3 N/mm²). Further controls limit the compression strength between 3 and 7 MPa; this guarantees indirectly that the cement treated base is not excessively fragile.

This study researched the effect of increased tensile resistance produced by the fibers; therefore, tests were in accordance with ASTM C 496-90. The tests were carried out on cylindrical specimens (L=177.8 mm, D=152.4 mm) placed on a horizontal axis, compressed between two diametrically opposed generatrixes, with a load gradient between 1.1 MPa/s and 2.2 MPa/s. The breaking, in absence of fibers, occurs according to an approximately plane surface, parallel to the direction of load application. The characteristics of the single fiber influence the final mechanical properties of the cement treated bases. The shape and dimensions (length and diameter) are very important both for the final performances of the composite material and for its workability. There are no particular difficulties with slenderness ratios less than 90-100. For higher values the mixture becomes heterogeneous with segregations and is difficult to mix. On the market there is a great variety of fibers available: round, square, rectangular, contorted, and barbed at the extremities, with rough or smooth surfaces. The shape primarily influences the pull-out resistance. The fiber used in this test had the following characteristics: lenght 60 mm; section 0,78 mm²; aspect ratio 60.

**Figure 1 Fibers used in the test**

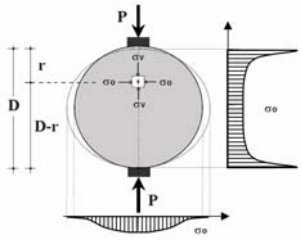


**Figure 2 Scheme of the stresses**

The stresses $\sigma_V$ and $\sigma_o$, applied to the cylindrical specimens (figure 2), are given by:

$$\sigma_V = \frac{2P}{\pi \cdot L \cdot D} \cdot \left\{ \left[ \frac{D^2}{r \cdot (D-r)} \right] - 1 \right\} \qquad (1) \qquad \sigma_o = \frac{2 \cdot P}{\pi \cdot L \cdot D} \qquad (2)$$

The tests were recorded with two digital camcorders. This allowed documentation of the evolution of cracking, the crack aperture, and the performance of the fibers. Furthermore, real-time measurements of applied load and controlled deformation were recorded to each frames. The displacements was evaluated, with a 64 μm resolution, from the analysis of two subsequent pictures.

The results are expressed as load-deformation curves for each different material composition, as the average of three specimens. Samples without fibers (group A and B), once having reached the breaking load, record high speeds of unloading; the curves are very steep and they show the typical performance of the cement treated base. The cracking develops in correspondence to the two load plates and progresses along the generatrix towards the barycenter of the specimen leading the sample to a fragile breaking. The breaking surfaces are well traced and regular.

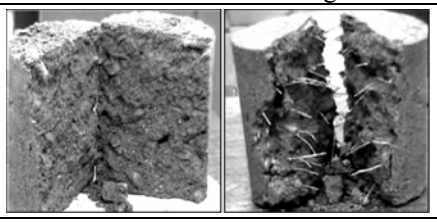

**Figure 3 Different breaking performance of un-reinforced and reinforced**

**Table 3 Average peak load value**

| **Materials** | **A** | **B** | **C** | **D** | **E** | **F** |
|---|---|---|---|---|---|---|
| **Load [KN]** | 9.10 | 15.30 | 10.93 | 15.33 | 10.83 | 17.40 |

The different quantity of cement brings an increase in the resistance, but also a higher fragility (Figure 3). The substantial difference determined by the presence of the fiber is given by the increase in the plastic phase. The fiber-reinforced samples at the end of the test are rarely separated. The breaking surface is not neatly exposed, only partially tied by the fibers placed orthogonally to the load. The softening phase of the fiber-reinforced samples show rapid load subsidences with steps of about 0.50 kN, due to the progressive loss of bond among the material and the fibers.

## 3. EXPERIMENTAL RESULTS

Comparisons have been made on the increase of the maximum resistance and the expansion of the plastic phase based on different average curves, evaluated as the area under the curves after the peak load. Comparison of the different groups shows that:

- for the reduced cement content (2.5%), the introduction of fibers (0.75%) results in a 15.70% increase in peak load. The most significant result is represented by the increase in the softness by 2.4 times;
- higher quantities of fiber (1.5%) result in a 14.29% increase in peak load, and a softness 3.4 times higher than the material with no fibers;
- in the material with 3.5% cement, the introduction of 0.75% fibers results in a slight 3.27% reduction of peak load, and a 59.34% increase in softness. By doubling the quantity of fiber, the peak increases by 12.42% compared to the un-reinforced material, whereas the softness results clearly increased (≈2.7 times);
- increasing the cement content from 2.5% to 3.5% increases the breaking load by 61.9% in the material with no fibers and by 59.3% in the material with 1.5% fibers.

The test was repeated considering the plastic area equal to 20% and 50% of the breaking load. The results obtained are shown in Table 4 and in Figure 6.

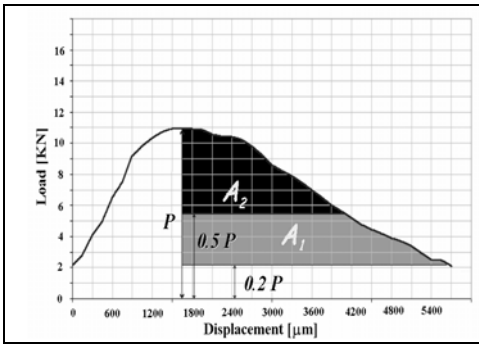


**Figure 5 The areas $A_1$ and $A_2$ assess the extent of the plastic phase**

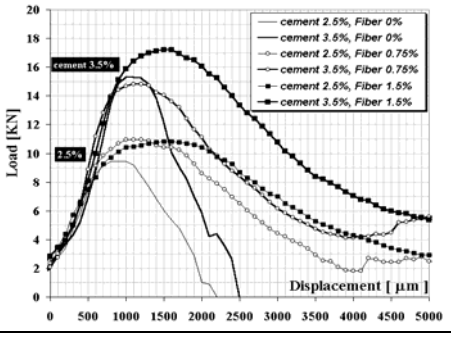


**Figure 6 Load curves for the six composite materials**

**Table 5 Difference among the plastic areas of the specimens**

| Cement 2,5% | 50% | 20% | Cement 3,5% | 50% | 20% |
|---|---|---|---|---|---|
| **A➔ C** | 183,33% | 208,30% | **B➔ D** | 97,06% | 198,87% |
| **A ➔ E** | 220,63% | 331,80% | **B ➔ F** | 183,54% | 319,59% |
| **D ➔ E** | 13,16% | 40,06% | **D ➔ F** | 43,89% | 40,43% |

In summary, the variation of the modulus of rupture following the introduction of the fiber is among 14% and 21%, while on average is equal to 46% if the quantity of cement passes from 2.5% to 3.5%. Better performance may be obtained by considering the deformation of the breaking. They are similar as the percentage of binder varies (max 16%), while they reach 54% in the specimens produced with 1.5% fibers. The material stiffness, Ec, varies remarkably as a function of both the quantity of fiber and the quantity of cement: on the average, 69% among the two different quantities of cement, and 32% in the fiber-reinforced specimens compared to those with no fiber. The following diagram shows the empirical results for $f_0$, $\varepsilon_0$, Ec

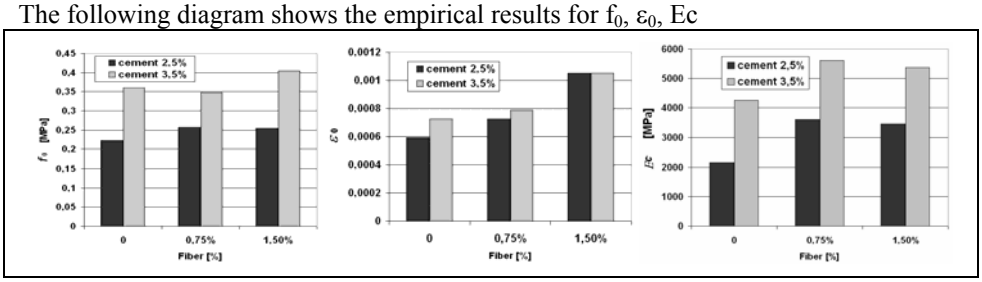


**Figure 7 Maximum tensile stress for the collapse (f0), deformation for the breaking (ε0), and rigidity module (Ec)**

## 4. FATIGUE IN CEMENT TREATED BASES

The assessment of the benefit of the fiber-reinforcement on the fatigue life of the material was carried out on the basis of a theoretical method which relates the envelope of the cycles of hysteresis and the σ–ε curve in tension. Fatigue is an irreversible process of damage to the material which can be triggered when the material is exposed

to a high number of stress cycles, even sharply less than the values of static strength. Concerning road superstructures, it is not usual for collapse to takes place after limits of static resistance have been overcome, whereas almost in every case the end of the life service represents fatigue phenomena, cracking and plastic deformation. The succession of stresses, even lower than 50% of the typical static resistance value determines the outbreak of the phenomenon. Fatigue breaking occurs as a particular ultimate limit state induced when the working load cycles limit is exceeded. This led, especially in the last ten years, to testing of superstructure criteria based on the real mechanism of cracking due to fatigue. This occurs with the decay of the macroscopic resistance characteristics, mainly that of deformability of the material. Decay depends on several elements, among which there are the range and the number of the load cycles, their average value and their frequency. The mechanisms that form the basis of the fatigue phenomenon in cement treated material can be schematized in this way:

- during laying, micro-cracks and cavities, mainly in the cement-aggregate interface, are produced. Other surfaces of discontinuity are caused by shrinkage and the thermal gradient. In the material, shrinkage cracking is surely the main cause of discontinuity, which is emphasized by the higher quantity of cement;
- when the material is subjected to stresses less than the fatigue limit resistance (30-40% of the static breaking load), these surfaces of discontinuity are not substantially modified. The $\sigma-\varepsilon$ curve remains almost linear and the fatigue does not occur;
- for higher stress values, the discontinuities increase, expanding until causing the progressive collapse by fatigue of the material;
- after the breaking has occurred, the pavement begins to loose its structural integrity and the cemented material, working with both reduced load bearing capacity and rigidity, transfers part of its structural function to the superior bitumen layers.

Therefore, it is important to have fatigue curves which link the material stresses to the number of cycles that cause the collapse. Figure 8 shows some of the models proposed for the decay of the fatigue in the cement compound.

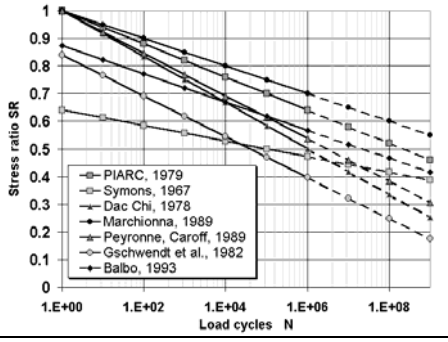


**Figure 8 Fatigue curves proposed for the cement treated materials**

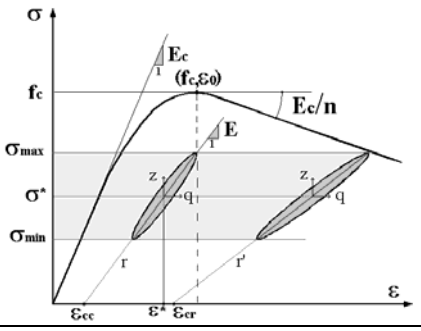


**Figure 9 Indirect tensile curve and cycles of hysteresis**

Different formulations were proposed to linearly relate the stress ratio (SR) to the logarithm of the number of the load cycles (N). The tests are valid in an elastic field, but permanent modifications and plastic readjustment inside the material cannot be excluded when studying the fatigue phenomenon. The concept of "Damage" defines

and quantifies the progress of the phenomenon as a function of the number of cycles and the value of the maximum stresses. Figure 8 shows different curves of fatigue for the cement treated bases. A simple damage law was proposed by Miner, as linear accumulation, for which the damage D is given by:

$$D = \sum_{1}^{s} \frac{n_i}{N_i} \qquad (3)$$

where $n_i$ is the number of cycles made for stress-block *i* of range $\Delta\sigma_i$ and $N_i$ is the number of cycles required to reach the breaking point of the same $\Delta\sigma_i$. The material reaches fatigue breaking when D=1.

## 5. MODEL FORMULATION

In the analysis of the fatigue life of the cemented material, models analogous to those for the cement concrete in tension were used both to obtain a valid method to define the stress-deformation relation and to trace the performance of hysteresis and the evolution of the stiffness until subsidence. In absence of references to compare the performance observed with the indirect tensile tests on the cement treated material, load-displacement curves were studied to assess the fatigue performance, also taking into account the softening phase. If static loads are applied when performing fatigue tests, oscillations would occur in the specimen and induce cycles of hysteresis.
The breaking, and subsequently, the number of cycles, is traced by the intersection of the load line with the plastic phase of the load-displacement curve, obtained with the indirect tensile test. Therefore, the intersection of the maximum stress ratio SR with descending segment of the σ–ε curve indicates a unique number of cycles to failure, $N_f$, proportional to the length of the segment. Assessing the different $N_f$ values of each material, an evaluation of the increase of their fatigue life was obtained.
A main reference system (ε, σ) was defined for the envelope curve, and one relative (q, z) for the cycles of hysteresis. Normalized values for tensile stress and deformation, z and q, are expressed as:

$$z = \frac{\sigma - \sigma^*}{f_c} \qquad q = \varepsilon - \varepsilon^* \quad (4)$$

in which σ* and ε* represent the average instantaneous tensile stress and deformation. With this scheme, the accumulated damage can be represented by the plastic deformation, $\varepsilon_{cc0,}$ according to the expression:

$$E = \frac{E_c}{(1 + \frac{2 \cdot \varepsilon_{cc0}}{\varepsilon_0})} = \lambda \cdot E_c \quad (5)$$

Subsidence due to fatigue occurs when the cycles of hysteresis reaches the descending segment of the envelope σ-ε curve in tension, and the permanent deformation becomes $\varepsilon_{cc}=\varepsilon_{cr}$. Also the value of $f_{ctm}$ decays. A proposed relation (Verna, Stelson, 1963.) is:

$$f_{ctm(N)} = f_{ctm}\left(1 - \frac{\log N}{11}\right) \quad (6)$$

On the basis of empirical data (R. Calzona, E. Dolora, 1996), the permanent deformation due to the fatigue in tension, in correspondence of the barycenter of the cycle of hysteresis, $\varepsilon_{cc0}$, is given by (k = 0.455 $10^{-6}$ and h = -0.56):

$$\varepsilon_{cc0} = k \cdot S_{cm} \cdot \Delta S_c \cdot N^h \cdot 10^{-6} \qquad (7)$$

with: $$S_{cm} = \frac{\sigma_{\max} + \sigma_{\min}}{2 f_{ctm(N)}} \qquad \Delta S_c = \frac{\sigma_{\max} - \sigma_{\min}}{f_{ctm(N)}} \qquad (8)$$

Finally, the number of the fatigue cycles is given (Park, 1990), by the relation:

$$N_f = \frac{12 \cdot \varepsilon_{cr}}{\left[\left(\frac{d\varepsilon_{cc}}{dN}\right)_1 + 4 \cdot \left(\frac{d\varepsilon_{cc}}{dN}\right)_2 + 2 \cdot \left(\frac{d\varepsilon_{cc}}{dN}\right)_3 + 4 \cdot \left(\frac{d\varepsilon_{cc}}{dN}\right)_4 + \left(\frac{d\varepsilon_{cc}}{dN}\right)_5\right]} \qquad (9)$$

where $\varepsilon_{cr}$ is the plastic deformation at the fatigue failure (by the envelope curve), and $d\varepsilon_{cc}/dN$ is determined in 5 points with the same interval of permanent deformation to $\varepsilon_{cr}$.

In the development of the previous model, the average of stress ratio, $\sigma/f_{ctm}$, is limited between 0.1 and 0.3. Given the permanent deformation in tension obtained by the relation for $\varepsilon_{cc0}$, it is possible to determine the value of $\varepsilon_{cr}$ by extrapolating the axis of the cycles of hysteresis with the progress of the number of cycles until intercepting the ε-axis. Then, discretizing its value in equal intervals and calculating at each interval the value of $d\varepsilon_{cc}/dN$, $N_f$ may be determined. The iteration of the calculation for different stress levels allows designing fatigue curves for each kind of material starting from the simple static indirect tensile test.

## 6. RESULTS FROM FATIGUE MODEL

Figure 10 shows the results obtained for a fiber content of 0.75% and a cement of 3.5%.

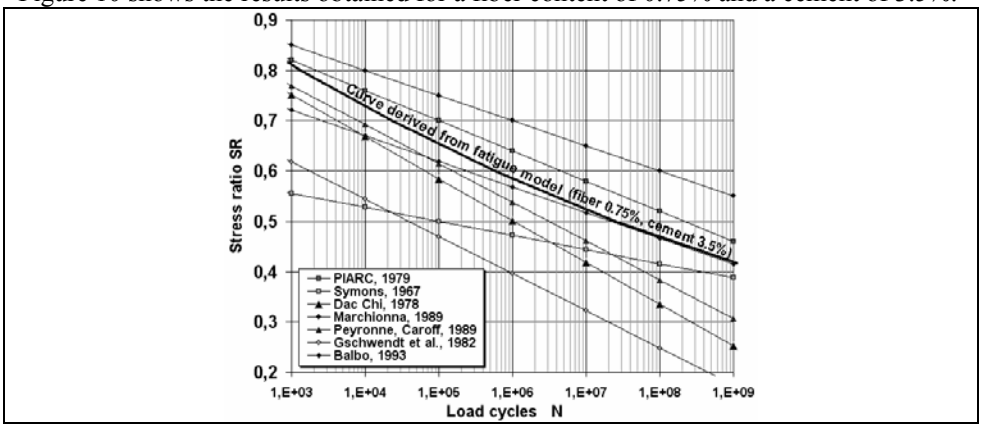


**Figure 10 Fatigue curve obtained by the model (fiber=0.75% and cement =3.5%)**

Given the stress-deformation by an indirect tensile test conducted statically until cracking occurs, and knowing the effective stress level in the material, it is possible to derive the number of load cycles which will determine the fatigue phenomenon. In

order to obtain a better approximation of the empirical results, the coefficients k and h in Equation 7 are equal to: k=7.8 $10^{-3}$, h= - 0.10.
The fatigue curves obtained for the six different materials (A-F) are shown in Figure 11.

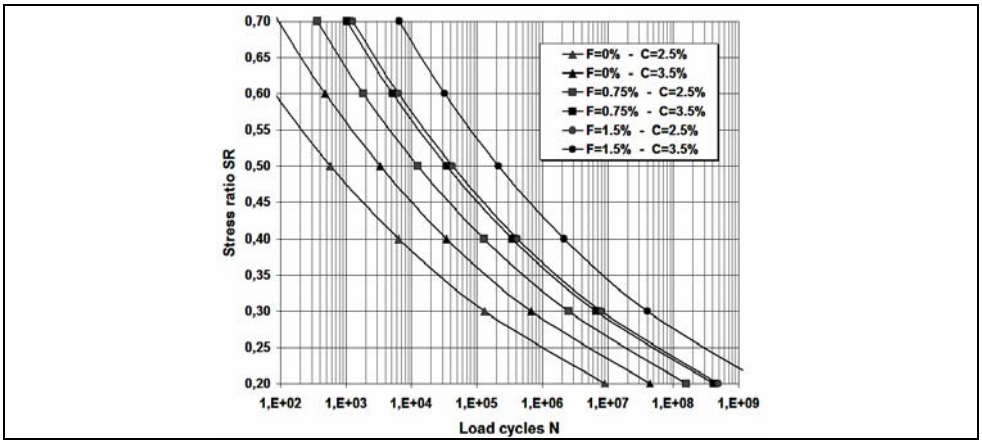


**Figure 11 Fatigue curves in the 6 different materials (A-F)**

Figure 11 shows that the performance of the cemented materials is improved with the introduction of the metallic fiber. Referring to SR=0.4, it is possible to assure that:

- there is a progressive improvement with material from type A to type F;
- using B as the reference material (without fibers and a typical quantity of cement), the fatigue service life of the F material is about 60 times higher, as shown in Table 6

**Table 6 Increment of fatigue life for 6 materials**

| **Material** | **A** | **B** | **C** | **D** | **E** | **E** |
|---|---|---|---|---|---|---|
| **Cement %** | 2.5 | 3.5 | 2.5 | 3.5 | 2.5 | 3.5 |
| **Fiber** kg/m$^3$ | 0 | 0 | 0.75 | 0.75 | 1.50 | 1.50 |
| **Rate vs B** | 0,18 | 1,00 | 3,72 | 10,00 | 12,16 | 62,17 |

- on average, with quantity of fiber being equal and cement content increasing from 2.5% to 3.5%, the number of load cycles at fatigue failure increases 4.41 times.
- fatigue life tends to increase as the stress ratio SR increases;
- the fatigue life of the specimens with 0.75% fiber increases approximately 15.13 times compared to the ones without fibers;
- the doubling of percentage of fiber (1.5%) allows a further increment of 4.74 times the number of load cycles before fatigue failure.

## 7. FIBER CORROSION

Despite the benefits presented, the potential of fiber-reinforced cement treated bases has not been adequately studied, probably because of the potential corrosion of the metallic fibers. In order to check the needed technologies for the laying of the material and the

actual level of corrosion of the fiber in working conditions, two empirical studies were made in the recently built main road, S.S. n. 125, in south-east Sardinia (Italy).
In March 2004, after two years of service, a series of core samples were collected from the study area and analyzed electrochemically in the laboratory. The results underlined the almost complete absence of corrosion and the presence of nearly intact fibers.
To extend the results of this study, chemical tests were conducted on intact fibers in different aggressive environments. Dissolved oxygen in water is considered the most dangerous corrosive agent for steel fibers. Along with this there are also other elements that strongly affect corrosion. For a pH < 2-3, the corrosive attack is extremely severe and leads to the rapid destruction of the exposed metal surface. Nevertheless it is extremely rare that water in contact with a cement treated aggregate has such acidic concentrations. Vice versa, for values of pH > 7, the corrosive process is strongly delayed or repressed with the formation of a film of oxide which is adhered and continuous and protects the underlying metal from further corrosive attack. The latter is the typical environment for fibers inside cement treated aggregates. In the tests carried out in the laboratory, the fibers had been exposed for an extended period (up to 180 days) to the action of three different solutions: water from the municipal supply (pH ≈ 7); an aqueous solution of HC1 10% (pH ≈ 3); and an aqueous solution containing cement in hydration (pH ≈ 10). The speed of corrosion of the steel may be assessed through the intensity of a supplied electrical current (See Figure 12). It is possible to pinpoint the existing corrosive process in the steel through measuring the potential of the battery.

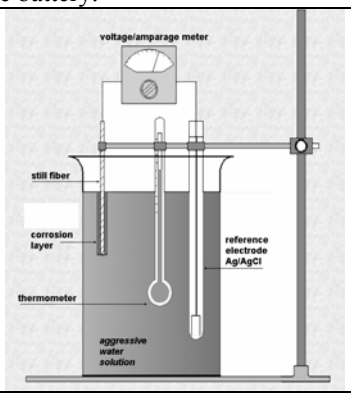


**Figure 12 Empirical device for the assessment of the degree of corrosion**

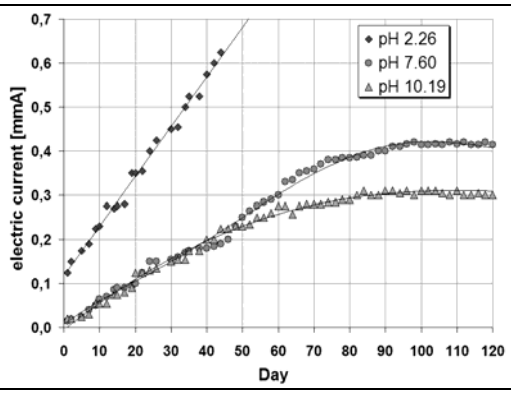


**Figure 13 Evolution of the corrosion of the fibers in solutions with different pH**

The curves of Figure 13 show the evolution of the corrosion phenomenon over time. The results are summarized as follows:

- in an acid environment the intensity of the current increases continuously with time, with a linear trend, and with a constant development of $H_2$. After about 28 days, the exposed fiber is completely corroded and the products of the corrosion are deposited at the bottom of the beaker;
- in an almost neutral environment (water of the municipal supply, pH ~7.6), the intensity of the current increases more slowly, and normalizes in about 90 days.

After the initial attack we have the formation of a compact film of oxide and hydroxide which decelerates the corrosion until it is stopped;

- in a basic environment, obtained adding the Portland cement to the solution, the corrosion progresses for the first 40 days in a way similar to that of the previous case, and then it reaches a stable state more rapidly, with a lower severity and diffusion. This is the situation occurring inside the cement treated aggregates.

The strong basic environment created inside the cement treated base remains unaltered even for long periods, considering the remarkable quantities of $Ca(OH)_2$ released during the hydration process of the clinker compounds, $C_2S$ and $C_3S$, present in the mass of hardened material. The readings up to 60 days, showing the intensity of the electrical current, indicate the continued increase of corrosion. After this period the phenomenon normalizes: in the graphic it is clear how the corrosive process then stops. In such conditions, with the extrapolation of the empirical curve, the corrosion may be assessed as approximately 0.15 mm after 50 years of fiber exposure, at pH = 10. The time is reduced to 4-5 years in an environment with pH = 7. Among the different mixtures studied, none were identified to have a higher performance, such as to have better protective characteristics of the steel fiber. In other words, there are not significant correlations between the granulometric and cement composition of the mixture and the corrosion of the fiber.

## 8. CONCLUSION

The results of the study show how the performance of the cement treated bases can be strongly improved through the use of metallic fibers. The fiber has various functions: increase in the softness of the cement treated base, as well as the elongation at rupture; redistribution of the stresses inside the material; limitation of the aperture of the cracks; increase in the fatigue life service; limitation of the initial higrothermic cracking during casting and ageing. In particular, research showed how the increase in the softness determines a significant increment in the fatigue resistance, as a function of the quantity of fiber. The number of load cycles at collapse increases by more than 15 times with a fiber content of 0.75% and more than 60 times with a content of 1.5%. The differences are even more remarkable as the working rate grows.

The empirical work was completed with the development of an analysis model of the fatigue life of the cement treated bases, in parallel with performance models developed on the concrete in tension. The method allows for tracing of the fatigue curve of a material on the basis of the stress-deformation relation obtained by an indirect tensile test, and for tracing of the evolution of the hysterises performance and of the stiffness until failure. The failure and, subsequently, the number of cycles, is indicated by the intersection of the axis of the cycle of hysteresis with the plastic field of the empirical curve. The advancement of this technology has been inhibited by the risk of potential corrosion of the fibers. The tests carried out in the laboratory and in situ show an unexpected integrity of the fibers due to the protection provided by a strongly basic environment created by the cement.

The chemical tests in the laboratory show how in such a situation the fiber suffers an initial attack with the formation of an oxide and hydroxide compact film which delays the corrosion until it stops it rapidly. Even core samples collected from the empirical

area highlight the presence of intact fibers after more than 2 years within the cement treated bases. A further limit to the spreading of the fiber-reinforced cement treated bases is their high cost. This can be overcome partially by using fibers with minimal mechanical characteristics and by reducing the fiber content to less than 1% in weight. This will not have a negative impact on final performance of compound material and will preserve the benefits. Finally, the advancement of this technology depends on the standardization of test methods and the improvement of current techniques for dispersion and mixing of fibers inside the cement treated bases.

## REFERENCES

ASTM C1018-97 Standard Test Method for Flexural Toughness and First-Crack Strength of Fiber-Reinforced Concrete (Using Beam With Third-Point Loading).

BALAGURU, P. N., AND SHAH, S. P. (1992). "Fiber Reinforced Cement Composites." McGraw Hill, Inc., New York.

CRAIG, R., SCHURING, J., COSTELLO, W., AND SOONG, L. (1987). "Fiber Reinforced Soil Cement." American Concrete Institute, SP-105, oaf. S. P. Shah, and G. B. Batson. pp. 119-139.

CAVEY, J. K., KRIZEK, R. J., SOBHAN, K., AND BAKER, W. H. (1995). "Waste Fibers in Cement-Stabilized Recycled Aggregate Base Course Material," Transportation Research Record 1486, Transportation Research Board, Washington, D.C., pp. 97-106.

CALZONA R, DOLORA E., (1996), "Fatica e decadimento dei materiali e delle strutture sottoposte ad azioni cicliche", Università Roma "Sapienza" Esagrafica, Roma.

KENNEDY, T. W., MOORE, R. K., AND ANAGNOS, J. N. (1971). "Estimations of Indirect Tensile Strengths for Cement-Treated Materials." Highway Research Record, Number 351, Highway Research Board, Washington, D. C.

KHALED SOBHAN, RAYMOND J. KRIZEK, STANLEY F. PEPPER, (1996), "Fiber-reinforced recycled crushed concrete as a stabilized base course for highway pavements", Proceedings of the First International Conference on Fiber Composites in Infrastructure, January 15-17, 1996, Tucson, Arizona, 1996, pp. 996-1011.

HOOVER, J. M., MOELLER, D. T., PITT, J. M., SMITH, S. G., AND WAINAINA, N. W. (1982). "Performance of Randomly Oriented, Fiber-reinforced Roadway Soils." Iowa DOT Project HR-211, College of Engineering, Iowa State University.

Park, Y.T. (1990) "Fatigue of concrete under random loading", Journal Str. Eng. N.11

THOMPSON, M. R. (1994). "High-Strength Stabilized Base Thickness Design Procedure." TRR N. 1440, Transportation Research Board, Washington, D. C. pp. 1-7.

VERNA, J.R AND STELSON, T.E. "Repeated loading effect on ultimate static strength of concrete beam", J. Amer. Concrete Inst, V. 60, n.6, June 1963.

## ACKNOWLEDGEMENT

We acknowledge Dr. F. Ruggieri of the ANAS for placing at our disposal the road section for the in situ research, and Fibrocev® which provided the fibers for the testing. In addition, we acknowledge Prof. G. Usai and the laboratory material testing of the DIS (Department of Structural Engineering), and the DICM (Department of Chemical and Material Engineering) of the University of Cagliari.